

Fig. 1. A lossy post in a rectangular waveguide.

conductor, k_c has the form [9]

$$k_c = \sqrt{\frac{\omega\mu\sigma}{2}} - j\sqrt{\frac{\omega\mu\sigma}{2}} \quad (4)$$

where σ is the conductivity of the post.

The free-space field due to the current density distribution of (3) is assumed to be

$$E_x^s = \sum_{n=-\infty}^{\infty} a_n H_n^{(2)}(kr) e^{jn\theta}. \quad (5)$$

Consider an elementary shell of radius r' and width dr' inside the post. The field due to the current distribution of this shell is assumed to be

$$dE_x^s(r') = \sum_{n=-\infty}^{\infty} a_n(r') H_n^{(2)}(kr) e^{jn\theta} dr'. \quad (6)$$

Then, $a_n(r')$ is related to a'_n as in [8]

$$a_n(r') = -a'_n \frac{k^2 \pi r' J_n(kr')}{2\omega\epsilon} \cdot \frac{J_n(k_c r')}{J_n(k_c r_o)}. \quad (7)$$

Integrating (6) with respect to r' over the interval (o, r_o) yields

$$\begin{aligned} a_n &= -a'_n \frac{k^2 \pi}{2\omega\epsilon} \int_o^{r_o} r' J_n(kr') \frac{J_n(k_c r')}{J_n(k_c r_o)} dr' \\ &= -a'_n \frac{\pi}{2\omega\epsilon} G_n \end{aligned} \quad (8)$$

where

$$G_n = \int_o^{kr_o} x J_n(X) \frac{J_n(\beta x)}{J_n(\beta kr_o)} dx \quad (9)$$

and

$$\beta = \frac{k_c}{k} = \sqrt{\frac{\sigma}{2\omega\epsilon}} (i - j). \quad (10)$$

The tangential component of the electric field on the surface can be obtained from (3)

$$E_x(r = r_o) = \frac{1}{\sigma} J_x(r = r_o) = \sum_{n=-\infty}^{\infty} \frac{a'_n}{\sigma} \cdot e^{jn\theta}. \quad (11)$$

Substituting (8) into (11) yields

$$E_x(r = r_o) = - \sum_{n=-\infty}^{\infty} \frac{2\omega\epsilon}{\pi\sigma G_n} a_n e^{jn\theta}. \quad (12)$$

The calculation of scattered fields proceeds as in [8]. The boundary condition can be expressed as

$$E_x^s(r = r_o) + E_x^i(r = r_o) = E_x(r = r_o).$$

This results in the matrix equation

$$[H][a] + [Z_L][a] = [c] \quad (13)$$

where $[H]$, $[a]$, and $[c]$ are given in [8]. The additional matrix $[Z_L]$ is a diagonal matrix; therefore, its entries are determined by

$$z_{nm} = \begin{cases} 0, & \text{for } n \neq m \\ \frac{2\omega\epsilon}{\pi\sigma G_n}, & \text{for } n = m. \end{cases} \quad (14)$$

As the conductivity σ approaches infinity, all the entries of matrix $[Z_L]$ go to zero and (13) reduces to that obtained in the lossless case.

The calculations of the transmission and reflection coefficients proceeds as in [8]

$$T = 1 + \frac{4}{E_o k' a} \sum_{n=-\infty}^{\infty} (-1)^n a_n \sin\left(\frac{\pi c}{a} - n\alpha\right) \quad (15)$$

$$\Gamma = \frac{4}{E_o k' a} \sum_{n=-\infty}^{\infty} a_n \sin\left(\frac{\pi c}{a} + n\alpha\right). \quad (16)$$

Note that the only difference between the lossless and lossy cases is the addition of the matrix $[Z_L]$ and the consequent modification of coefficients $[a]$ as determined by matrix equation (13). In general, the entries of the loss matrix $[Z_L]$ are determined by (14), where G_n is determined by (9).

For good conductors, the calculation is simplified since the magnitude of the complex number β is large, i.e., $|\beta| = \sqrt{\sigma/\omega\epsilon} \gg 1$. For large arguments, the Bessel function is approximated as follows [10]:

$$J_n(u) = \sqrt{\frac{2}{\pi u}} \cos\left(u - \frac{n\pi}{2} - \frac{\pi}{4}\right), \quad \text{for } |u| \gg 1. \quad (17)$$

In the integrand of (9), the ratio $J_n(\beta x)/J_n(\beta kr_o)$ has a significant value only as x approaches kr_o .

Applying (17) and formulas $\sin(jx) = j \sinh x$ and $\cos(jx) = \cosh x$, it is found that

$$\begin{aligned} G_n &= kr_o J_n(kr_o) \int_o^{kr_o} e^{j\beta(x-kr_o)} dx \\ &= kr_o J_n(kr_o) \frac{1 - e^{-j\beta kr_o}}{j\beta} \end{aligned} \quad (18)$$

where $\beta = \beta_1 - j\beta_1$ and $\beta_1 = \sqrt{\sigma/2\omega\epsilon}$. Because $\beta_1 kr_o \gg 1$, then $e^{-j\beta kr_o} \approx 0$. Therefore

$$G_n = \frac{kr_o J_n(kr_o)}{j\beta}. \quad (19)$$

Substituting (19) into (14) yields

$$z_{nm} = \begin{cases} 0, & \text{for } n \neq m \\ \frac{2\omega\epsilon\beta_1}{\pi\sigma kr_o J_n(kr_o)} \cdot (1 + j), & \text{for } n = m. \end{cases} \quad (20)$$

The total power dissipated in the post is obtained as follows (field quantities are rms rather than peak):

$$P_d = \iiint \sigma |E_x|^2 d\tau = \iiint \frac{1}{\sigma} |J_x|^2 d\tau. \quad (21)$$

Substituting (3) into (21) yields

$$P_d = \frac{\sqrt{2} \pi b r_o}{\sigma |k_c|} \sum_{n=-\infty}^{\infty} |a'_n|^2. \quad (22)$$

III. WALL LOSSES

The wall losses can be treated by perturbational methods. Recall that the fields due to a uniform filament located at $y = y', z = z'$ in a rectangular waveguide (Fig. 1) are [4]

$$E_x = \sum_{m=1}^{\infty} -\frac{jk\eta I}{\Gamma_m a} \sin \frac{m\pi y'}{a} \sin \frac{m\pi y}{a} e^{-\Gamma_m |z-z'|} \quad (23)$$

$$H_y = -\sum_{m=1}^{\infty} \operatorname{sgn}(z-z') \frac{I}{a} \sin \frac{m\pi y'}{a} \sin \frac{m\pi y}{a} e^{-\Gamma_m |z-z'|} \quad (24)$$

$$H_z = -\sum_{m=1}^{\infty} \frac{I}{a} \frac{m\pi}{\Gamma_m a} \sin \frac{m\pi y'}{a} \cos \frac{m\pi y}{a} e^{-\Gamma_m |z-z'|} \quad (25)$$

where $\Gamma_1 = jk'$, $\Gamma_m = \sqrt{(m\pi/a)^2 - k^2}$, $m \geq 2$.

Equations (24) and (25) are the Green's function of the magnetic field in rectangular waveguide. Using these equations, we can obtain the scattered magnetic fields due to the volume current-density distribution inside the post

$$H_y^s = -\sum_{m=1}^{\infty} \frac{r_o}{a} \int_0^{2\pi} \operatorname{sgn}(z - r_o \sin \theta) \cdot \sum_{n=-\infty}^{\infty} a''_n e^{jn\theta} \sin \frac{m\pi(c + r_o \cos \theta)}{a} \cdot \sin \frac{m\pi y}{a} e^{-\Gamma_m |z - r_o \sin \theta|} d\theta \quad (26)$$

$$H_z^s = -\sum_{m=1}^{\infty} \frac{r_o}{a} \frac{m\pi}{\Gamma_m a} \int_0^{2\pi} \cdot \sum_{n=-\infty}^{\infty} a''_n e^{jn\theta} \sin \frac{m\pi(c + r_o \cos \theta)}{a} \cdot \cos \frac{m\pi y}{a} e^{-\Gamma_m |z - r_o \sin \theta|} d\theta \quad (27)$$

where a''_n is the coefficient of the equivalent surface current density of the post, $\{a''_n\}$ is related to $\{a_n\}$ by [11]

$$a''_n = -\frac{2\omega\epsilon}{k^2 \pi r_o J_n(kr_o)} a_n \quad (28)$$

and to $\{a'_n\}$ by $a''_n = a'_n/jk_c$. The incident magnetic fields are obtained from (1), let $E_o = 1$

$$H_y^i = \frac{k'}{\omega\mu} \sin \frac{\pi y}{a} e^{-jk'z} \quad (29)$$

$$H_z^i = -\frac{j\pi}{\omega\mu a} \cos \frac{\pi y}{a} e^{-jk'z}. \quad (30)$$

The power dissipated on the walls can be calculated by

$$P_d = \mathcal{R} \iint |\mathbf{H}^i + \mathbf{H}^s|^2 ds \quad (31)$$

where \mathcal{R} is the intrinsic wave resistance; however, for a good conductor it is [9]

$$\mathcal{R} = \sqrt{\frac{\omega\mu}{2\sigma}}. \quad (32)$$

We now consider the numerical calculation of the magnetic fields. First, consider the left-hand side wall. The total tangential component of the magnetic fields is ($y = 0, H_y = 0$)

$$H = H_z = H_{zd} + H_{zh} \quad (33)$$

where H_{zd} stands for the dominant mode

$$H_{zd} = \frac{-j\pi}{\omega\mu a} e^{-jk'z} + \frac{j\pi r_o}{k' a^2} \int_0^{2\pi} \sum_{n=-\infty}^{\infty} a''_n e^{jn\theta} \cdot \sin \frac{\pi(c + r_o \cos \theta)}{a} e^{-jk'|z - r_o \sin \theta|} d\theta \quad (34)$$

and H_{zh} stands for the higher order modes

$$H_{zh} = -\sum_{m=2}^{\infty} \frac{m\pi r_o}{\Gamma_m a^2} \int_0^{2\pi} \sum_{n=-\infty}^{\infty} a''_n e^{jn\theta} \sin \frac{m\pi(c + r_o \cos \theta)}{a} \cdot e^{-\Gamma_m |z - r_o \sin \theta|} d\theta. \quad (35)$$

H_{zd} can be evaluated by truncation ($-N \leq n \leq N$). When $|z| \geq r_o$, (34) can be reduced to [11]

$$H_{zd} = -\frac{j\pi T}{\eta ka} e^{-jk'z}, \quad \text{for } z \geq r_o \quad (36)$$

$$H_{zd} = -\frac{j\pi}{\eta ka} (e^{-jk'z} + \Gamma e^{jk'z}), \quad \text{for } z \leq -r_o \quad (37)$$

where T and Γ are the transmission and reflection coefficients, respectively.

Note that (36) represents a traveling wave and (37) represents a standing wave.

The convergence of the series in (35), which is slow in the post region, can be improved by separating H_{zh} into two parts, i.e.,

$$H_{zh} = H_{zh}^{(1)} + H_{zh}^{(2)} \quad (38)$$

where

$$H_{zh}^{(1)} = \int_0^{2\pi} \sum_{n=-\infty}^{\infty} a''_n e^{jn\theta} \sum_{m=2}^{\infty} \left(-\frac{r_o}{a} \right) e^{-m\pi/a|z - r_o \sin \theta|} \cdot \sin \frac{m\pi(c + r_o \cos \theta)}{a} d\theta \quad (39)$$

$$H_{zh}^{(2)} = \int_0^{2\pi} \sum_{n=-\infty}^{\infty} a''_n e^{jn\theta} \cdot \sum_{m=2}^{\infty} \frac{r_o}{a} \left[e^{-m\pi/a|z - r_o \sin \theta|} - \frac{m\pi/a}{\Gamma_m} e^{-\Gamma_m |z - r_o \sin \theta|} \right] \cdot \sin \frac{m\pi(c + r_o \cos \theta)}{a} d\theta. \quad (40)$$

Equation (39) can be simplified as

$$H_{zh}^{(1)} = -\frac{r_o}{2a} \int_o^{2\pi} d\theta \sum_{n=-\infty}^{\infty} a_n'' e^{jn\theta} \left[\frac{f_1(\theta) - f_2(\theta)}{f_3(\theta) - f_4(\theta)} \right] \quad (41)$$

where

$$\begin{aligned} f_1(\theta) &= \exp\left(-\frac{\pi}{a}|z - r_o \sin \theta|\right) \sin \frac{2\pi(c + r_o \cos \theta)}{a} \\ f_2(\theta) &= \exp\left(-\frac{2\pi}{a}|z - r_o \sin \theta|\right) \sin \frac{\pi(c + r_o \cos \theta)}{a} \\ f_3(\theta) &= \cosh \frac{\pi(z - r_o \sin \theta)}{a} \\ f_4(\theta) &= \cos \frac{\pi(c + r_o \cos \theta)}{a} \end{aligned}$$

Equation (40) is a rapid convergent series; therefore, it can be evaluated by truncation.

Similarly, for the right-hand side wall ($y = a$), we have the following results:

$$H_z = H_{zd} + H_{zh}^{(1)} + H_{zh}^{(2)} \quad (42)$$

where

$$\begin{aligned} H_{zd} &= \frac{j\pi}{\omega\mu a} e^{-jk'z} - \frac{j\pi r_o}{k' a^2} \int_0^{2\pi} \\ &\quad \cdot \sum_{n=-\infty}^{\infty} a_n'' e^{jn\theta} \sin \frac{\pi(c + r_o \cos \theta)}{a} e^{-jk'|z - r_o \sin \theta|} d\theta \end{aligned} \quad (43)$$

when $|z| \geq r_o$, (43) reduces, respectively, to

$$H_{zd} = \frac{j\pi T}{\eta ka} e^{-jk'z}, \quad \text{for } z \geq r_o \quad (44)$$

$$H_{zd} = \frac{j\pi}{\eta ka} (e^{-jk'z} + \Gamma e^{jk'z}), \quad \text{for } z \leq -r_o \quad (45)$$

$$H_{zh}^{(1)} = -\frac{r_o}{2a} \int_o^{2\pi} d\theta \sum_{n=-\infty}^{\infty} a_n'' e^{jn\theta} \left[\frac{f_1(\theta) + f_2(\theta)}{f_3(\theta) + f_4(\theta)} \right] \quad (46)$$

$$\begin{aligned} H_{zh}^{(2)} &= \int_o^{2\pi} \sum_{n=-\infty}^{\infty} a_n'' e^{jn\theta} \sum_{m=2}^{\infty} (-1)^m \frac{r_o}{a} \\ &\quad \cdot \left[e^{-\frac{m\pi}{a}|z - r_o \sin \theta|} - \frac{m\pi}{\Gamma_m a} e^{-\Gamma_m|z - r_o \sin \theta|} \right] \\ &\quad \cdot \sin \frac{m\pi(c + r_o \cos \theta)}{a} d\theta. \end{aligned} \quad (47)$$

We now consider the top and bottom wall losses per unit length. Let P_d denote the power dissipated per unit length on the top or bottom wall. Then

$$P_d = \mathcal{R} \left[\int_o^a H_y H_y^* dy + \int_o^a H_z H_z^* dy \right] \quad (48)$$

where H_y is determined by (26) and (29), H_z is determined by (27) and (30), and \mathcal{R} is determined by (32).

Calculations of the two terms of (48) are similar; consider the second term only—the first term is evaluated in [11].

Since $\{\sin m\pi Y/a\}$ is an orthogonal set over the interval (o, a) , hence

$$\int_o^a H_z H_z^* dy = \int_o^a H_{zd} H_{zd}^* dy + \int_o^a H_{zh} H_{zh}^* dy \quad (49)$$

where subscripts d, h denote the dominant and higher order modes, respectively.

Note that orthogonality is maintained for top wall, but not for side wall, losses.

Substituting (27) and (30) into (49) yields

$$\begin{aligned} \int_o^a H_{zd} H_{zd}^* dy &= \frac{\pi^2}{2\omega^2\mu^2 a} + \frac{r_o^2}{2a} \\ &\quad \cdot \frac{\pi^2}{k'^2 a^2} \left| \int_o^{2\pi} J_s(\theta) \sin \frac{\pi c_o(\theta)}{a} e^{-jk'z_o(\theta)} d\theta \right|^2 \\ &\quad - \frac{\pi^2 r_o}{k' \omega \mu a^2} \operatorname{Re} \left[e^{jk'z} \int_o^{2\pi} J_s(\theta) \right. \\ &\quad \left. \cdot \sin \frac{\pi c_o(\theta)}{a} e^{-jk'z_o(\theta)} d\theta \right] \end{aligned} \quad (50)$$

$$\begin{aligned} \int_o^a H_{zh} H_{zh}^* dy &= \frac{r_o^2}{2a} \int_o^{2\pi} d\theta J_s(\theta) \int_o^{2\pi} d\phi J_s^*(\phi) \\ &\quad \cdot \sum_{m=2}^{\infty} \left(\frac{m\pi}{\Gamma_m a} \right)^2 \sin \frac{m\pi c_o(\theta)}{a} \\ &\quad \cdot \sin \frac{m\pi c_o(\phi)}{a} e^{-\Gamma_m[z_o(\theta) + z_o(\phi)]} \end{aligned} \quad (51)$$

where $J_s(\theta)$ is the equivalent surface current density distribution on the post; it can be obtained by integrating (3) with respect to r from o to r_o . The result is

$$J_s(\theta) \triangleq \sum_{n=-\infty}^{\infty} a_n'' e^{jn\theta} = \sum_{n=-\infty}^{\infty} \frac{a_n'}{jk_c} e^{jn\theta} \quad (52)$$

and

$$\begin{aligned} c_o(x) &= c + r_o \cos x \\ z_o(x) &= |-r_o \sin x| \end{aligned} \quad (53)$$

Equation (50) can be evaluated by using truncation. As in (51), there still are convergence problems. In order to overcome this difficulty, we again separate the series in (51) into two parts.

Let

$$\begin{aligned} M_z(\theta, \phi) &= \sum_{m=2}^{\infty} \left(\frac{m\pi}{\Gamma_m a} \right)^2 \sin \frac{m\pi c_o(\theta)}{a} \\ &\quad \cdot \sin \frac{m\pi c_o(\phi)}{a} e^{-\Gamma_m[z_o(\theta) + z_o(\phi)]} \\ &= M_1(\theta, \phi) + M_2(\theta, \phi) \end{aligned} \quad (54)$$

where

$$\begin{aligned} M_1(\theta, \phi) &= \sum_{m=2}^{\infty} \\ &\quad \cdot \sin \frac{m\pi c_o(\theta)}{a} \sin \frac{m\pi c_o(\phi)}{a} e^{-\frac{m\pi}{a}[z_o(\theta) + z_o(\phi)]} \end{aligned} \quad (55)$$

$$\begin{aligned} M_2(\theta, \phi) &= \sum_{m=2}^{\infty} \sin \frac{m\pi c_o(\theta)}{a} \sin \frac{m\pi c_o(\phi)}{a} \\ &\quad \cdot \left\{ \left(\frac{m\pi}{\Gamma_m a} \right)^2 e^{-\Gamma_m[z_o(\theta) + z_o(\phi)]} - e^{-\frac{m\pi}{a}[z_o(\theta) + z_o(\phi)]} \right\}. \end{aligned} \quad (56)$$

Series (56) converges rapidly; hence, it can be evaluated by truncation. A closed form of the series (55) can be obtained

$$M_1(\theta, \phi) = \frac{1}{4} \left[\frac{e^{-\frac{\pi}{a}z_o^+} \cos \frac{2\pi c_o^-}{a} - e^{-\frac{2\pi}{a}z_o^+} \cos \frac{\pi c_o^-}{a}}{\cosh \frac{\pi z_o^+}{a} - \cos \frac{\pi c_o^-}{a}} - \frac{e^{-\frac{\pi}{a}z_o^+} \cos \frac{2\pi c_o^+}{a} - e^{-\frac{2\pi}{a}z_o^+} \cos \frac{\pi c_o^+}{a}}{\cosh \frac{\pi z_o^+}{a} - \cos \frac{\pi c_o^+}{a}} \right] \quad (57)$$

where

$$\begin{aligned} z_o^+ &= z_o(\theta) + z_o(\phi) \\ c_o^+ &= c_o(\theta) + c_o(\phi) \\ c_o^- &= c_o(\theta) - c_o(\phi). \end{aligned} \quad (58)$$

As in the case of side wall losses, the expressions of the dominant terms of top (or bottom) wall losses can also be reduced when $|z| \geq r_o$. The results are

$$\int_o^a H_d H_d^* dy = \frac{a|T|^2}{2\eta^2}, \quad \text{for } z \geq r_o \quad (59)$$

$$\int_o^a H_d H_d^* dy = \frac{a}{2\eta^2} [1 + |\Gamma|^2 - 2 \cos 2\alpha R_e(\Gamma e^{j2k'z})],$$

for $z \leq -r_o$. (60)

IV. EQUIVALENT CIRCUIT

The equivalent circuit for the lossless case can be represented by a "T" network consisting of a shunt reactance X_a , and two series reactance X_b . The shunt and series reactances X_a and X_b , respectively, can be related to the reflection and transmission coefficients by

$$-jX_b = \frac{1 + \Gamma - T}{1 - \Gamma + T} \quad (61)$$

$$jX_a = \frac{1}{1 - \Gamma - T} - \frac{1}{2} + j\frac{X_b}{2} \quad (62)$$

where T and Γ are the transmission and reflection coefficients, respectively. In the lossless case, the right-hand sides of (61) and (62) are purely imaginary. For lossy posts, we must modify the equivalent circuit by replacing jX_a and $-jX_b$ by Z_a and Z_b , respectively, as shown in Fig. 2. The shunt and series impedances can also be related to the reflection and transmission coefficients by [11]

$$Z_b = \frac{1 + \Gamma - T}{1 - \Gamma + T} \quad (63)$$

$$Z_a = \frac{1}{1 - \Gamma - T} - \frac{1}{2} - \frac{1}{2}Z_b. \quad (64)$$

In Section II, we have shown the exact solutions of transmission and reflection coefficients for the lossy post case. Applying the solutions of T and Γ to (63) and (64), we obtain the parameters Z'_a and Z'_b of the equivalent

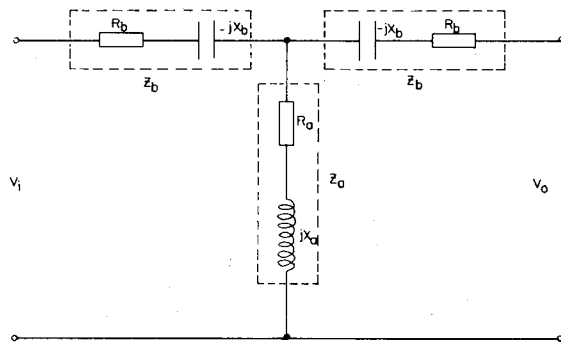


Fig. 2. Equivalent circuit for a lossy post.

circuit. Let

$$Z'_a = R'_a + jX'_a \quad (65a)$$

$$Z'_b = R'_b - jX'_b \quad (65b)$$

and

$$X'_a = X_a + \Delta X'_a \quad (66a)$$

$$X'_b = X_b - \Delta X'_b \quad (66b)$$

where X_a and X_b are the shunt and series reactances, respectively, for the lossless case.

Numerical calculations show that, for posts which are good conductors

$$R'_a = \Delta X'_a \ll X_a \quad (67a)$$

$$R'_b = \Delta X'_b \ll X_b \quad (67b)$$

in agreement with Wheeler's incremental inductance rule [12]. The results of our numerical calculations satisfy (67) within better than one percent. The wall losses can be taken into account as follows. The wall losses are separated into two parts, the losses due to the dominant waveguide mode, and the losses due to the difference between the total wall loss and the dominant mode wall losses.

The effect of the dominant mode wall losses can be treated by consideration of the waveguide as a lossy transmission line. The attenuation constant is given by [9]

$$\alpha = \frac{\bar{\mathcal{P}}_d}{2\bar{\mathcal{P}}_f}$$

where $\bar{\mathcal{P}}_f$ is the time-average power flow, and $\bar{\mathcal{P}}_d$ is the time-average power dissipated per unit length in the guide walls due to the dominant mode fields. The calculations of $\bar{\mathcal{P}}_f$ and $\bar{\mathcal{P}}_d$ have been treated in Section III.

The effect of the difference between the total wall losses and the dominant mode wall losses can be taken into account by modifying the parameters of the equivalent circuit.

Assume the parameters Z_a and Z_b should be modified as follows:

$$Z_a = R'_a + R''_a + j(X_a + \Delta X'_a + \Delta X''_a) \quad (68a)$$

$$Z_b = R'_b + R''_b - j(X_b - \Delta X'_b - \Delta X''_b) \quad (68b)$$

where R'_a , R'_b , $\Delta X'_a$, and $\Delta X'_b$ are due to the post losses, and R''_a , R''_b , $\Delta X''_a$, and $\Delta X''_b$ are due to the difference

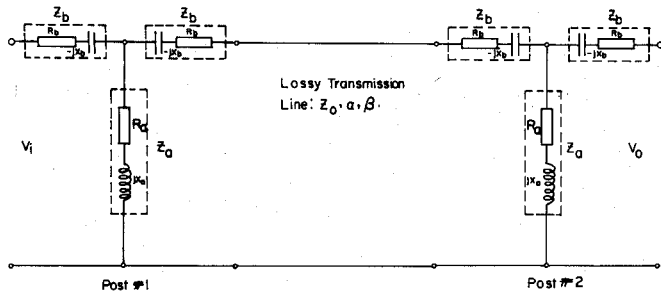


Fig. 3. Equivalent circuit for a lossy post array and lossy walls.

TABLE I
THE MODIFIED EQUIVALENT CIRCUIT PARAMETERS (FOR LOSSY POST)

$\lambda/a = 1.20$		$f = 10^9$		$\sigma = 5.80E+7$	
d/a	$\Delta X'_a$	R'_a	$\Delta X'_b$	R'_b	
0.100	0.180E-4	0.180E-4	0.727E-5	0.726E-5	
0.200	0.612E-5	0.614E-5	0.122E-4	0.122E-4	
0.300	0.229E-5	0.228E-5	0.166E-4	0.166E-4	
$\lambda/a = 1.20$		$f = 10^{10}$		$\sigma = 5.80E+7$	
d/a	$\Delta X'_a$	R'_a	$\Delta X'_b$	R'_b	
0.100	0.570E-4	0.570E-4	0.230E-4	0.230E-4	
0.200	0.194E-4	0.194E-4	0.386E-4	0.386E-4	
0.300	0.723E-5	0.724E-5	0.524E-4	0.524E-4	
$\lambda/a = 1.20$		$f = 10^{11}$		$\sigma = 5.80E+7$	
d/a	$\Delta X'_a$	R'_a	$\Delta X'_b$	R'_b	
0.100	0.180E-3	0.180E-3	0.727E-4	0.724E-4	
0.200	0.612E-4	0.614E-4	0.122E-3	0.122E-3	
0.300	0.229E-4	0.229E-4	0.166E-3	0.166E-3	

between the total wall losses and the dominant mode wall losses.

For a good conductor, the losses are small. Therefore, the changes of the parameters, in first-order approximation, should be proportional to the lossy power, i.e.,

$$\frac{R''_a}{R'_a} = \frac{R''_b}{R'_b} = \frac{\Delta X''_a}{\Delta X'_a} = \frac{\Delta X''_b}{\Delta X'_b} = \frac{P''}{P'} \quad (69)$$

where P'' is the excess wall losses (the difference between the total wall losses and the dominant mode wall losses) and P' is the post losses. The complete equivalent circuit may thus be specified and is shown in Fig. 3.

V. RESULTS

As noted previously, a rigorous solution has been obtained for the lossy post case. Fig. 2 shows the modified equivalent circuit obtained. Additional resistive elements have been added in both series and shunt elements. Table I shows typical equivalent circuit data for copper posts. Note that (67) is satisfied. Furthermore, for good conductors, the ratio R'_a/R'_b varies only slightly with conductivity and frequency and is primarily a function of d/a . This ratio is shown in Fig. 4. Fig. 5 shows computed transmission coefficient data for a lossy two-element post filter, as a function of conductivity. The parameter n may be chosen as desired to yield different center frequencies.

The wall losses have been calculated using a perturbational method. Computed results are shown in Figs. 6(a)–(c)

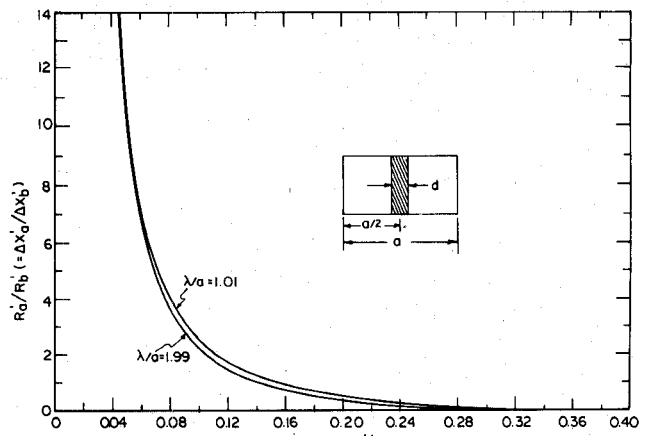
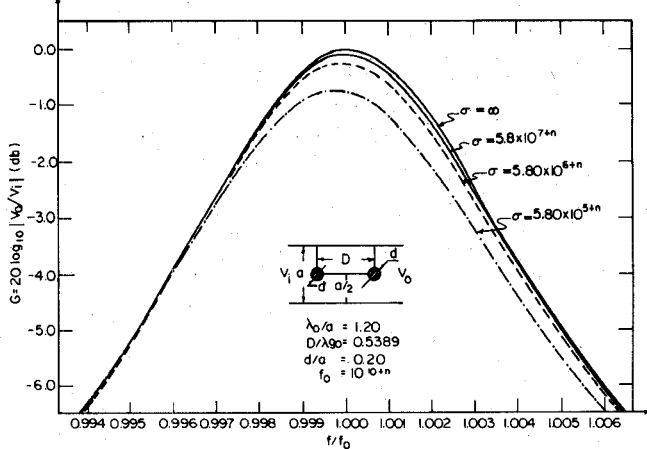
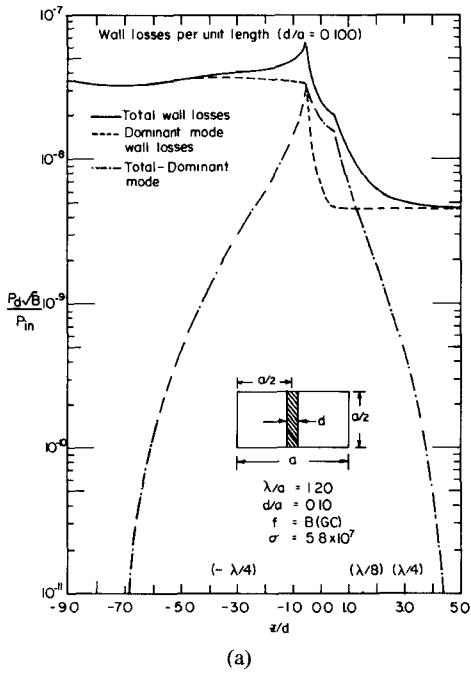
Fig. 4. Resistance ratio (R'_a/R'_b).

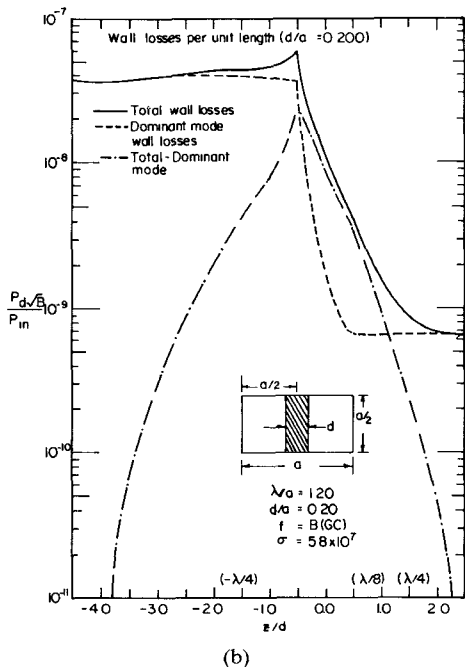
Fig. 5. Filter response (transmission coefficient) of a lossy post array.

for three different post sizes ($d/a = 0.10, 0.20, 0.30$). The total wall losses per unit length, including side, top, and bottom walls, have been calculated as a function of position z relative to the post axis. Calculations have been made assuming that the post and walls are copper and $b = a/2$.

The dominant mode wall losses have also been computed and the difference between the total wall losses and the dominant mode (total minus dominant mode) is also plotted in Fig. 6. The dominant mode losses may, of course, be calculated very simply and so the difference between total and dominant mode losses is of interest. Note that the wall losses of the various modes are not orthogonal and thus the difference of total and dominant mode losses cannot necessarily be ascribed solely to higher order mode losses. Fig. 6 shows the wall losses per unit length for a single post. Table II shows the corresponding (integrated) wall losses over a length L of waveguide on either side of the post axis. This represents an integration of the data of Fig. 6. The integration extends over three distinct regions ($z < -d/2$, $|z| \leq d/2$, and $z \geq d/2$) and involves side, top, and bottom walls of the waveguide as well as post losses. L varies from $d/2$ to $\lambda_g/2$ to show the effect of various post spacings. All losses in Table II are normalized to incident power. Note that the total minus



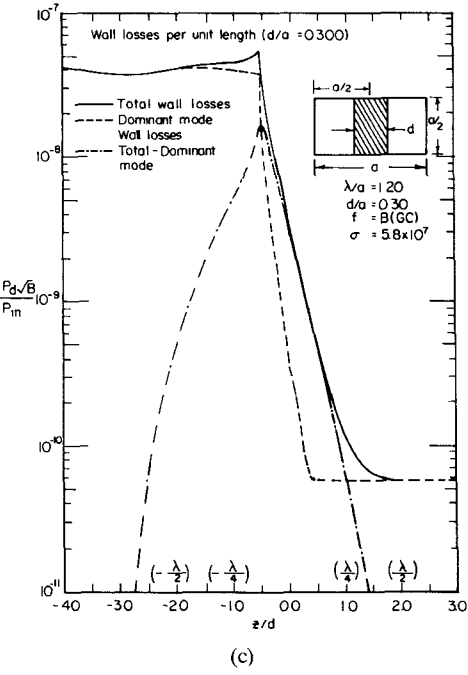
(a)



(b)

Fig. 6. Wall losses per unit length. (a) $d/a = 0.10$, (b) $d/a = 0.20$, (c) $d/a = 0.30$.

dominant losses appear to have reached a value close to their peak value at $\lambda_g/4$, which agrees with what one would expect relative to higher order mode losses. The total losses are represented by the sum of the post losses and the total wall losses. Note that the total wall losses and post losses are comparable in some cases. If the post wire is constructed of a lossy material such as brass, then post losses would increase proportionately. Thus, post losses may be comparable to wall losses or may even exceed them. Note particularly that the total minus dominant losses are relatively small compared to the sum of post and dominant mode losses. The ratio varies from 10.2 to 18.5



(c)

Fig. 6. (Continued)

TABLE II
RELATIVE WALL LOSSES

($\lambda_g/a = 1.20$, $f = 50\text{GHz}$, $\sigma = 5.80 \times 10^7$)					
$d/a = 0.10$ (post losses = 0.254×10^{-3})					
L	$d/2$	$\lambda_g/8$	$\lambda_g/4$	$3\lambda_g/8$	$\lambda_g/2$
Total wall losses	0.498E-4	0.186E-3	0.329E-3	0.459E-3	0.578E-3
Dominant mode wall losses	0.152E-4	0.106E-3	0.236E-3	0.363E-3	0.482E-3
Total-Dominant	0.346E-4	0.800E-4	0.938E-4	0.962E-4	0.962E-4
$d/a = 0.20$ (post losses = 0.215×10^{-3})					
L	$d/2$	$\lambda_g/8$	$\lambda_g/4$	$3\lambda_g/8$	$\lambda_g/2$
Total wall losses	0.519E-4	0.131E-3	0.276E-3	0.411E-3	0.532E-3
Dominant mode wall losses	0.153E-4	0.716E-4	0.200E-3	0.330E-3	0.451E-3
Total-Dominant	0.366E-4	0.596E-4	0.768E-4	0.809E-4	0.814E-4
$d/a = 0.30$ (post losses = 0.192×10^{-3})					
L	$d/2$	$\lambda_g/8$	$\lambda_g/4$	$3\lambda_g/8$	$\lambda_g/2$
Total wall losses	0.421E-4	0.742E-4	0.218E-3	0.355E-3	0.480E-3
Dominant mode wall losses	0.136E-4	0.373E-4	0.162E-3	0.293E-3	0.418E-3
Total-Dominant	0.285E-4	0.369E-4	0.561E-4	0.615E-4	0.625E-4

percent for $L \leq \lambda_g/2$. Thus, if one were to approximate losses by the sum of post losses and dominant mode losses only, the error would be less than 18.5 percent in this region. This approximation is represented in Fig. 3. One may then readily cascade such circuits to analyze the lossy characteristics of an array of posts. This method would yield reasonably accurate results and would be relatively easy to apply. For a more accurate representation, we need to consider the total minus dominant mode (excess) term which may be taken into account by utilizing (69).

VI. CONCLUSIONS

Lossy inductive posts in a lossy rectangular waveguide have been treated. Post losses are taken into account by a rigorous moment-method solution which yields a modified

equivalent circuit. Wall losses are taken into account by perturbational methods. Total wall losses are separated into dominant and excess losses. Dominant losses are included in a lossy transmission-line model. Excess losses may be neglected or incorporated by further modification in the equivalent circuit.

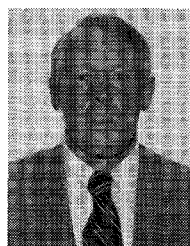
REFERENCES

- [1] D. S. Saxon, *Notes on Lectures by Julian Schwinger: Discontinuities in Waveguides*, Ann Arbor, MI: University Microfilms.
- [2] N. Marcuvitz, *Waveguide Handbook* (M.I.T. Rad. Lab. Series, vol. 10). New York: McGraw-Hill, 1951, pp. 257-262.
- [3] G. Craven and L. Lewin, "Design of microwave filters with quarter-wave couplings," *J. Inst. Elec. Eng.*, vol. 103(b), pp. 173-177, 1956.
- [4] L. Lewin, *Theory of Waveguides*. New York: Wiley, 1975.
- [5] E. A. Mariani, "Designing narrow-band triple-post waveguide filters," *Microwaves*, vol. 4, pp. 93-97, 1965. See also "Design of narrow-band, direct-coupled waveguide filters using triple-post inductive obstacles," Tech. Rep. ECOM-2566, U.S. Army Electronics Command, Fort Monmouth, NJ, Mar. 1965.
- [6] A. V. Moschinskiy and V. K. Berezovskiy, "An exact solution of the problem of scattering of the H_{10} mode on a circular cylindrical inhomogeneity in a rectangular waveguide," *Radio Eng. Electron. Phys.*, vol. 22, pp. 18-22, July 1977.
- [7] T. A. Abele, "Inductive post arrays in rectangular waveguide," *Bell Syst. Tech. J.*, vol. 57, no. 3, pp. 577-594, Mar. 1978.
- [8] P. G. Li, A. T. Adams, Y. Leviatan, and J. Perini, "Multiple-post inductive obstacles in rectangular waveguide," *IEEE Trans. Microwave Theory Tech.*, vol. 32, pp. 365-373, Apr. 1984.
- [9] R. F. Harrington, *Time-Harmonic Electromagnetic Fields*. New York: McGraw-Hill 1961, pp. 50, 66.
- [10] Jahnke-Emde-Lösch, *Tables of Higher Functions*, 6th Ed. New York: McGraw-Hill, 1960, pp. 146-147.
- [11] P. G. Li, A. T. Adams, J. Perini, and Y. Leviatan, "Multiple-post inductive obstacles in rectangular waveguide," Report TR-83-20, Department of Electrical and Computer Engineering, Syracuse University, NY, Dec. 1983.

- [12] H. A. Wheeler, "Formulas for the skin effect," *Proc. IRE*, pp. 412-424, Sept. 1942.



Ping Guan Li was born in 1945 in Changde County, Fukien Province, China. He graduated from the Department of Radio-Electronics, Tsinghua University, People's Republic of China, in February, 1968. He came to the United States in 1981 for postgraduate studies at Syracuse University, where he received the M.S. degree in August 1982, and the Ph.D. degree in May 1984.



Arlon Taylor Adams (SM'72) was born in Bottineau, ND, on April 26, 1931. He received the B.A. degree in applied science from Harvard University, Cambridge, MA, in 1953, and the M.S. and Ph.D. degrees in electrical engineering in 1961 and 1964, respectively, both from the University of Michigan, Ann Arbor.

He served as a Line Officer in the Atlantic Destroyer Fleet from 1953 to 1957, and until 1959 he was employed by Sperry Gyroscope Company, Long Island, NY. From 1959 to 1963,

he was a Graduate Research Associate at the University of Michigan, Ann Arbor. In 1963, he joined the faculty of Syracuse University, Syracuse, NY, where he is presently Professor of Electrical Engineering. His primary concerns in research are in numerical methods for antennas and microwaves. He is the author of a textbook on electromagnetic theory and coauthor of a textbook on electromagnetic compatibility.

Dr. Adams is a member of Phi Kappa Phi, Eta Kappa Nu, and the American Association of University Professors.

Complex Propagation Constants of Bent Hollow Waveguides with Arbitrary Cross Section

IMITSUNOBU MIYAGI

Abstract — An integral representation of the complex propagation constant β has been derived from Maxwell's equations for cylindrical, hollow, bent, oversized waveguides with uniform curvature and with arbitrary cross sections. The method makes the calculations much simpler than the conventional method, i.e., the characteristic-equation method, although it has not yet been tried for three-dimensional bent waveguides.

Manuscript received April 18, 1984; revised July 17, 1984.

The author is with the Research Institute of Electrical Communication, Tohoku University, Sendai 980, Japan.

I. INTRODUCTION

FOLLOW WAVEGUIDES are important transmission media for CO_2 laser light because they are expected to be able to carry high power [1]. One of the serious problems of hollow waveguides is the increased loss due to bends. Therefore, waveguide structures with small bending losses should be designed for the realization of a high-powered delivery system [1]-[4].